Experimental Brain Research (2020) 238:121–138
https://doi.org/10.1007/s00221-019-05679-9

RESEARCH ARTICLE

Muscle activities in similar arms performing identical tasks reveal the neural basis of muscle synergies

Laura Pellegrino[1] · **Martina Coscia**[2,3] · **Maura Casadio**[1]

Received: 17 July 2019 / Accepted: 7 November 2019 / Published online: 5 December 2019

Abstract

Are the muscle synergies extracted from multiple electromyographic signals an expression of neural information processing, or rather a by-product of mechanical and task constraints? To address this question, we asked 41 right-handed adults to perform a variety of motor tasks with their left and right arms. The analysis of the muscle activities resulted in the identification of synergies whose activation was different for the two sides. In particular, tasks involving the control of isometric forces resulted in larger differences. As the two arms essentially have identical biomechanical structure, we concluded that the differences observed in the activation of the respective synergies must be attributed to neural control.

Keywords Upper limb · Robotic evaluation · Reaching · Electromyography

Introduction

Every time we perform a voluntary movement, the central nervous system (CNS) activates and coordinates a multitude of muscles, including thousands of motor units. How the CNS successfully manages such complexity has been a matter of discussion for many years. Bernstein (Bernstein 1967) proposed a theory addressing this question, which is currently considered the main point of reference: he hypothesized that the CNS's burden is reduced because the motor system uses low-level discrete elements, or motor modules, to construct a large repertoire of movements (Bernstein 1967). Experiments on animal models (Mussa-Ivaldi and Bizzi 2000; Giszter et al. 2007; Hart and Giszter 2010) supported Bernstein's theory, showing that the discrete elements that it posits are muscle synergies, neurophysiological entities whose combination is orchestrated by the motor cortical areas and the afferent sensory systems (Bizzi and Cheung 2013). Muscle synergies engaged in the execution of motor tasks have been identified in human subjects through the analysis of electromyographic (EMG) activity (Lee and Seung 2001; Tresch et al. 2006). The result of the simultaneous activation of a few muscle synergies via descending or afferent pathways is supposed to produce the complex EMG patterns observed in the limb's muscles (Bizzi and Cheung 2013). Several studies on humans (Zardoshti-Kermani et al. 1995; d'Avella et al. 2003; Ivanenko et al. 2004; Cappellini et al. 2006; d'Avella et al. 2006; Ting and McKay 2007; Cheung et al. 2009a; Tropea et al. 2013; Barroso et al. 2014) support the hypothesis that muscle synergies extracted from the factorization of EMG signals reveal underlying patterns in muscle activity reflecting different levels of neural functions (Bizzi and Cheung 2013). However, Kutch et al. found biomechanical evidence of muscle synergies in a cadaveric human hand. Kutch et al. observed the muscle tensions in response to a sequence of pulls applied to the hand tendons and assumed that each muscle is independently instructed to resist length change (Kutch and Valero-Cuevas 2012).

Communicated by Francesco Lacquaniti.

Martina Coscia and Maura Casadio contributed equally as senior authors.

Electronic supplementary material The online version of this article (https://doi.org/10.1007/s00221-019-05679-9) contains supplementary material, which is available to authorized users.

✉ Maura Casadio
maura.casadio@unige.it

[1] Department of Informatics, Bioengineering, Robotics and Systems Engineering, University of Genoa, Via Opera Pia 13, 16145 Genoa, Italy

[2] Bertarelli Foundation Chair in Translational Neuroengineering, Ecole Polytechnique Federale de Lausanne, Lausanne, Switzerland

[3] Wyss Center for Bio- and Neuroengineering, Geneva, Switzerland

Consistent observations were obtained by extracting muscle synergies from the estimated muscle activity of a musculoskeletal model (Neptune et al. 2009; Kutch and Valero-Cuevas 2011; Ranganathan and Krishnan 2012; Steele et al. 2015). Constraints arising from the selected task and/or limb biomechanics could force couplings among muscles (Neptune et al. 2009; Kutch and Valero-Cuevas 2011, 2012; Ranganathan and Krishnan 2012; Steele et al. 2015). These studies stimulated a debate about the evidence that muscle synergies extracted from the factorization of EMG signals are basic motor modules representing a neural control strategy or are a mere by-product of simultaneous muscle activations due to biomechanical and/or task constraints. Bizzi and Cheung addressed this point in a review of experimental evidence (Bizzi and Cheung 2013). Animal studies revealed that muscle synergies are encoded in cortical neurons (Overduin et al. 2012; Batzianoulis et al. 2017). However, so far no studies with human subjects have been specifically designed to address whether muscle synergies extracted from multiple EMG signals could reveal their neural origin, excluding the possibility that task and/or limb biomechanics influenced the results.

Conceptually this could be demonstrated via intracortical recording or micro stimulation of motor cortical areas, as it has been done in monkeys (Overduin et al. 2012). However, these invasive procedures cannot be applied on healthy humans, and other less invasive technologies, such as transcranical magnetic stimulation and electroencephalography, might not have enough spatio/temporal resolution or would require extensive signal processing.

Alternatively, a simple experimental condition to reveal the influence of neural control on muscle synergies in humans would be to compare muscle synergies extracted from the factorization of EMG signals within each individual between two similar limbs controlled in a different way from the CNS, performing identical tasks. In this condition, muscle synergies features that differ between sides would reflect neural control, while muscle synergies features that are preserved between sides might depend also on other factors, such as biomechanics or task constraints. Therefore, we hypothesized that neural control features in upper limb muscle synergies can be revealed comparing the two upper body sides executing the same tasks in individuals with defined handedness.

We all experience handedness in everyday life as the tendency to prefer the use of one of the two limbs in performing motor tasks (Annett 1970, 2002; Bagesteiro and Sainburg 2002; Diederichsen et al. 2007). Much evidence shows that handedness results from differences in the neural control of the limbs, and it is characterized by specific neuro-motor features (Corballis 1983; Tan 1989; Semmler and Nordstrom 1998; Volkmann et al. 1998; Goble and Brown 2008). Differences between sides have been observed at different levels of the CNS, including the motor units firing rate (Adam et al. 1998), muscle activity and fatigue (Bagesteiro and Sainburg 2002; Farina et al. 2003), sensory-motor pathways (Friedli et al. 1987; Sathiamoorthy and Sathiamoorthy 1990), spinal and corticospinal tract (Tan 1989; Semmler and Nordstrom 1998), and cortical representations (Volkmann et al. 1998). The difference in neural control of upper limbs could be related to the cerebral hemisphere controlling each side, since there is evidence (Leib et al. 2018) that haptic processing is affected by laterality in the brain. While the origin of the difference of neural control between sides is still under investigation, it is widely accepted that handedness, when present, underlies a difference of neural control.

It is also known that upper limb laterality occurs at biomechanical level, such as in bone dimension (Auerbach and Ruff 2006) and muscle fiber composition (Fugl-Meyer et al. 1982). However, the small differences between upper limbs at the biomechanical level can be reasonably considered negligible in comparison to the differences in neural control when performing arm reaching movements. Also, they should not impact the estimation of muscle synergies as demonstrated by the possibility to identify similar muscle synergies across individuals (d'Avella et al. 2003; Ivanenko et al. 2004; Cappellini et al. 2006; d'Avella et al. 2006; Ting and McKay 2007; Cheung et al. 2009b; Tropea et al. 2013; Barroso et al. 2014) despite the inter-individual anatomical variability.

Therefore, if the CNS modulates a linear combination of basic motor modules identified as muscle synergies (coordinated muscle groups) to generate and control movements (Santello 2002; d'Avella et al. 2003; Osu et al. 2003; Ivanenko et al. 2004; d'Avella et al. 2006; Freitas et al. 2006; Ting and McKay 2007; Cheung et al. 2009a; Alessandro et al. 2013; Bizzi and Cheung 2013; Barroso et al. 2014; Berger and d'Avella 2014), we expect these synergies to be sensitive to differences in neural control of the two upper limbs in a population with defined (equal) handedness performing arm reaching movements.

We can assume that most of the differences between sides that can be observed in motor behavior are only related to neural control, as the limbs on the two sides have almost identical mechanical structure and it is possible to execute equal tasks with both arms. Therefore, it is possible to isolate the neural control contribution from the other components known to impact muscle synergies extracted from the factorization of EMG signals, such as biomechanical and task constraints, and determine if and how neural control is reflected in muscle synergies obtained from the factorization of EMG signals.

Only one small study (including ten young healthy subjects) previously investigated the effect of handedness on muscle synergies during the execution of planar wide and tight circular movements (Duthilleul et al. 2015). It

suggested a task-related difference in the muscle synergies of the two arms: the muscle synergies were generally similar between sides during the execution of planar wide circular movements, while during the execution of fine movements (i.e., planar tight circular movement), the dominant arm presented an additional synergy with respect to the non-dominant arm.

Here, we investigated upper limb performance and muscle synergies in a large population of right-dominant healthy adults performing planar movements and exerting controlled isometric forces with their right dominant (R) and left (L) arm in different mechanical environments. We included different mechanical environments and movement directions to increase variability in motor activation patterns (Steele et al. 2015). We found significant differences between the activation profiles of muscle synergies of the two arms during planar reaching movements. This difference increased when subjects performed an isometric force task. Muscle synergy analysis revealed that the CNS of right-dominant subjects adopts different control strategies for reaching with the right-dominant or the left limb, supporting our original hypothesis. Our results suggest that the activation of muscle synergies extracted from the factorization of upper limb EMG signals could directly reflect neural control. They also demonstrate that although tasks and biomechanical constraints impact muscle synergies, these can also reveal neural control if these constraints are well controlled in the experimental design.

Materials and methods

Subjects and ethical approval

Forty-one healthy adults (20 males and 21 females; 55 ± 12 years) were enrolled in the present study. They did not have any evidence or known history of postural, skeletal or neurological diseases, and exhibited normal joint range of motion and muscle strength. All subjects completed a short questionnaire based on the Edinburgh Medical Research Council handedness scale (Oldfield 1971). All subjects were right-handed (Edinburgh test: 91.5 ± 11.3 SD) and had no problems of visual integrity, i.e., they could clearly see the information about the target and the cursor positions displayed on the computer screen.

The study was approved by two local Ethical Committees (Comitato Etico ASL 3 Genovese 15/04/2013 Registro ASL 13/13 and Comitato Etico Regionale Liguria, 06-10-2014, 201REG2014) and conformed to the ethical standards of the 1964 Declaration of Helsinki. Each subject provided written informed consent to participate in the study and to publish individual data.

Procedure

Subjects performed four reaching tasks by controlling a cursor on a computer screen with upper limb movements or with the force applied by their limb. Specifically, the protocol consisted of the three movement tasks and one force task characterized by different mechanical environments:

- free space (FS): the subject's hand moved unimpeded by external forces (impedance of the environment ~ 0);
- assistive force (AF): a constant force field attracted the hand of the subjects toward the peripheral target (force amplitude: 5 N with an additional velocity-dependent viscous field with damping coefficient: 7 Nm/s);
- resistive force (RF): an elastic force field attracted the hand of the subject toward the center of the workspace (linear spring with stiffness coefficient of 15 N/m and with an additional velocity-dependent viscous field with damping coefficient: 7 Nm/s), generating a force field opposed to the subject motion to the peripheral target;
- rigid constrain (IF): the planar manipulandum was blocked in its central position in this case, the subjects applied isometric forces in different directions.

In all tasks, subjects grasped the handle of a planar robotic manipulandum (Casadio et al. 2006). The handle of the manipulandum included a fixed-force sensor (Gamma SI 13010, ATI Industrial Automation Inc.). In all tasks, the subjects were assuming the same posture or positioning and were instructed to perform the task with the upper limb. Differences across tasks were due to the different forces that were provided by the planar manipulandum.

Subjects were seated on a chair and the position of the seat was adjusted in such a way that the arm remained approximately horizontal at the shoulder level; the movements were restricted to the horizontal plane, with gravity compensation. A 19" LCD computer screen, positioned vertically in front of the subjects, about 1 m away at eye level, was used to display the current position of the hand and the targets. The cursor (green circle, 0.5 cm radius) correspondent to the position or the force generated by the hand was continuously displayed during the execution of the task. The targets were positioned in 8 directions (0°, 45°, 90°, 135°, 180°, 225°, 270°, 315°) equally spaced from a central target; see, Fig. 1. The targets (green circle, 1 cm radius) were positioned at 14 cm distance from the center, correspondent to 14 cm in the movement tasks and 10 N in the isometric force task. In particular, for the IF task, the displacement of the cursor was proportional to the input force (displacement = Kp force with Kp = 1.4 cm/N). Since the robot could have limitations into providing a rigid constraint with impedance control, the sensor connected to the handle was rigidly locked into the table. In all conditions, the

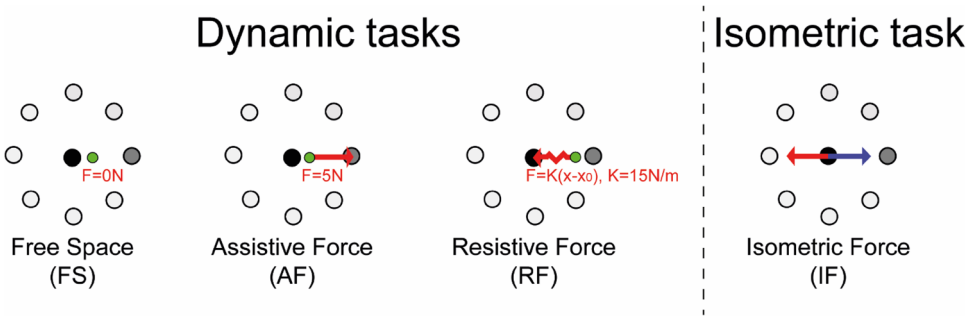

Fig. 1 Experimental protocol in the dynamic tasks; the black dot represents the starting target, the grey dot the target to reach, and the green dot the hand position. The red arrows indicate the force exerted by the robot. In the isometric task the blue arrow represents the force exerted by the subject while the red is the opposing force of the environment (force sensor)

central target and the central position of the robot workspace were aligned to the sagittal midline of the body.

In each task, the targets were presented ten times (80 center-out movements) in a random order. Each target was presented again only after all eight targets had been reached. Therefore, subjects performed a total of 80 × 4 (4 tasks) = 320 center-out movements for each arm. In each trial, the target appeared only when the subjects were in the central target position. After the subjects reached the target, the target disappeared after that the cursor stayed inside the target for 5 s, and a new target appeared.

Muscle activity was recorded with surface electrodes for EMG using the CometaWavePlus system (Cometa Srl, Cisliano, Milan, Italy). Electrodes were placed according to the guidelines of the Surface Electromyography for the Non-Invasive Assessment of Muscles European Community project (SENIAM) (Hermens et al. 2000) and to Anatomical guidelines (Perotto and Delagi 2005).

Surface EMG signals were recorded using superficial Ag–AgCl electrodes (AMBU N00S, electrodes 30 × 22 mm) from the following 14 upper limb muscles: Triceps Brachii long head (TB-long),triceps Brachii lateral head (TB-lat), Biceps Brachii short head (BB-short), Biceps Brachii long head (BB-long), brachioradialis (BRAD), pronator teres (PRON), infraspinatus (INFR), latissimus dorsi (LAT), upper trapezius (TRAP), rhomboid major (RHOM), pectoralis major (PECT), anterior deltoid (DELT-ant), medial deltoid (DELT-mid) and posterior deltoid (DELT-post). EMG electrode placement was performed according to recommendations for minimizing cross talk from adjacent muscles (Hermens et al. 2000) Also, the absence of cross talk among muscles was tested through visual inspection of the EMG signals while performing suitable movements at the moment of the electrode placement (Washabaugh and Krishnan 2018).

The hand order was randomized across subjects and the different tasks were presented in random order within each arm. Subjects could rest as long as they needed between tasks, otherwise the protocol required a break of 2 min between each task. The experimental sessions lasted about 2 h.

Data analysis

When comparing the two arms, we considered equivalent directions that corresponded in joint coordinates. In the endpoint space, the left-hand trajectories and the directions of action of muscle activities and synergies were mirrored at the midline to be compared with the corresponding right-hand trajectories and muscle directions. Thus, the target directions indicated in the text and figures as 315°, 0°, 45° corresponded to rightward movements of the R-hand and leftward movements of the L-hand, viceversa the target directions 135°, 180°, 225° corresponded to leftward movements of the R-hand and rightward movements of L-hand.

Kinematics analysis

Movement and force trajectories were sampled at 60 Hz and smoothed using a sixth order Savitzky–Golay filter (cutoff frequency: ~ 11 Hz for the movement signals and ~ 8 Hz for the force signals), which was also used to estimate the subsequent time derivatives of the trajectory (speed, acceleration and jerk). The onset of the cursor movement was defined as the first time instance when its speed exceeded the 10% of the maximum peak. The movement ended when the cursor was inside the target and the speed underwent and remained under the same threshold (Casadio et al. 2008). We focused our analysis on the center-out movements.

We computed the following performance indicators:

- Average speed (m/s): average speed of movement towards the peripheral targets.
- Jerk index (adimensional): the square root of the jerk (norm of the third time derivative of the trajectory), averaged over the entire movement duration and normalized

with respect to duration and path length (Teulings et al. 1997).

- 100-ms aiming error (°): the angular difference between the target direction and the actual movement direction, estimated in the first 100 ms of the movement (Casadio et al. 2007).
- End-point error (m): the distance between target position and cursor position when the speed fell below 10% of the maximum speed for the first time (Liu et al. 2011)
- Aspect ratio (adimensional): the maximum lateral distance from a straight line joining the start and end of the movement divided by the length of that line. It is a measure of the path curvature (Danziger and Mussa-Ivaldi 2012).

EMG pre-processing

Raw EMG signals were acquired at 2 kHz and processed off-line using a set of custom MATLAB routines; more specifically, we band-pass filtered (30–550 Hz), rectified and low-pass filtered at 10 Hz to obtain the EMG envelope time series(Cheung et al. 2009b, 2012). To correct the EMG-amplitude from differences in electrode placement, data from each muscle was normalized to the median value of activation obtained considering the EMG of that muscle recorded in all tasks. This normalization is robust against high-amplitude spikes arising from noise (Cheung et al. 2009b).

Analysis of muscle activation

The normalized EMG envelopes were segmented into trials corresponding to single center-out movement. For each trial, we considered a time window starting 250 ms before the movement onset (Flanders 1991) and ending with the movement termination.

The average speed in the L arm resulted similar to the average speed of the R arm in each task, as shown in Fig. 3e. For this reason, the normalized EMG envelope of each trial was resampled on 100 time points, and then averaged across the repetitions in the same direction, to compare the modulation of the EMG data collected in the four tasks and for the two arms (Coscia et al. 2014, 2015).

To compare the shape of the resampled normalized EMG envelopes between the R and L arms, we computed the Pearson correlation of the activity of each muscle between sides ($r_{\text{EMG-BETWEEEN-ARM}}$) in each task, i.e., we compared the resampled normalized EMG envelopes related to the R(L) arm of each subject with those of the L(R) arm of the other subjects (Coscia et al. 2014; Pellegrino et al. 2018). As reference value to assess the degree of similarity between sides, we calculated the degree of similarity across subjects within each side, computing the ''r'' values intra-arm. Specifically, we compared using the Pearson correlation coefficient the resampled normalized EMG envelopes of the R arm muscles across subjects and we repeated the same procedure for the L side, as described in (Pellegrino et al. 2018). The value obtained for the two arms were similar and therefore we used and reported their averaged value.

Analysis of muscle synergies

Extraction

For each subject, arm, and task, we used the non-negative matrix factorization (NMF) algorithm (Lee and Seung 2001) to extract muscle synergies from a matrix including the resampled normalized EMG envelopes related to the eight directions averaged across repetitions.

The NMF algorithm linearly decomposes the EMG envelopes in a defined number of positive components or muscle synergies, each composed of an activation profile (H) and a weight coefficient (W). The activation profile H represents the activation of each muscle synergy, and the weight coefficient W represents the participation of each muscle in each synergy (Cheung et al. 2009b; Roh et al. 2013; Tropea et al. 2013). Mathematically, the output of the algorithm (i.e., the normalized EMG envelopes, M) is the following:

$$M = \sum_{i=1}^{s} W_i * H_i \tag{1}$$

where S is the number of the muscle synergies, W_i is each weight coefficient, and H_i is each activation coefficient.

The combination of activation profiles and weight coefficients describe the muscle synergies (Ting and McKay 2007) according to Eq. 1. Given M as matrix including the normalized EMG envelopes, the matrix W reports for each column the weight coefficient of each muscle synergies, and H, the matrix where each row reports the activation profile for each synergy.

The NMF algorithm was based on the minimization of the "Euclidian distance" between the M and the combination of W and H.

To minimize the possibility that the iterative algorithm converged to a local and not a global minimum, we repeated the extraction 50 times and we selected the solution explaining the highest overall amount of variance (Cheung et al. 2009b; Roh et al. 2012). Synergy extraction was repeated with the number of synergies ranging from one to the number of recorded muscles: we obtained 14 sets of muscle synergies for each subject in each task and arm.

Estimation of the dimensionality

To determine the number of synergies, we combined two different methods based on the inspection of the R^2 curve.

R^2 represents the percentage of total variation of the EMG envelopes accounted for by the selected synergies. More specifically, the variance R^2 was computed as:

$$R^2 = 1 - \frac{\mathrm{SSE}}{\mathrm{SST}} = 1 - \frac{\sum s \sum_{k=1}^{k_s} ||m^s(t_k) - \sum_i c_i^s W_i(t_k - t_i^s)||^2}{\sum s \sum_{k=1}^{k_s} ||m^s(t_k) - \bar{m}||^2} \quad (2)$$

where SSE is the sum of the squared residuals, and SST is the sum of the squared residual from the mean activation vector ($\bar{m}$), i.e., the total variation multiplied by the total number of samples, t_k is the time of the kth sample in each trial; and c_i^s and t_i^s are the amplitude and timing coefficients for the ith synergy in trial s (d'Avella et al. 2006). For the first method, we computed the minimum number of synergies that achieved a $R^2 > 90\%$ (d'Avella et al. 2006). The second method was based on the detection of a change in slope of the R^2 curve. A series of linear regressions were performed on the portions of the curve included between the N-synergy ($N = 1$–14) and its last point (i.e., 14th synergy). N was then selected as the minimum value for which the mean squared error of the linear regression was less than 10^{-4} (Berger and d'Avella 2014). In case of a mismatch between the two criteria, the larger N was chosen (Roh et al. 2013; Berger and d'Avella 2014). For each task and side, we established this number as the rounded average across subjects.

Synergy similarity

The muscle synergies as output of the NMF algorithm are usually obtained not in the same order across subjects, tasks and sides. To match muscle synergies, we looked at the similarity of the weight coefficients, in terms of maximum normalized scalar product (d'Avella et al. 2003). To order muscle synergies across subjects, tasks and arms with respect to the same reference, we defined a "global reference system" for each task, as following. For each task, we pulled together the weight coefficients of muscle synergies of all subjects and arms. Then, we used a hierarchical cluster analysis calculating the Minkowski distance between vectors in each dataset using the pdist function ($p = 3$) and then we grouped the vectors linking pairs of weight coefficients that were in close proximity (similarity) using the linkage function (Ward option). Finally, we determined groups of similar weight coefficients according to a proximity threshold using the cluster function (Cheung et al. 2009b). For each task, the number of clusters specified for this technique was the same as the number of muscle synergies: 5 synergies for the FS, AF, and RF conditions and 4 synergies for the IF condition. The global reference system of weight coefficients for each task was obtained by averaging the synergy vectors within each cluster (Coscia et al. 2014; Pellegrino et al. 2018). Then, muscle synergies of each subject and arm were ordered according to the similarity of their weight coefficients to the global reference system for each task (Coscia et al. 2014; Pellegrino et al. 2018).

Specifically, the synergy vectors of each subject, task and arm were matched to the set of reference synergies, sequentially considering their normalized scalar products from the highest to the lowest.

The scalar product between the weight coefficient vectors normalized to their Euclidean norm (DOT) was also adopted to define a measure of the degree of similarity in the structure of two homologous muscle synergies (Cheung et al. 2005; d'Avella et al. 2006). With this metric, we evaluated the similarity of W between R and L arm in each task ($\mathrm{DOT}_{\mathrm{BETWEEN\text{-}ARM}}$).

Finally, to compare the shape (i.e., waveform) of the activation profile coefficients, we used the Pearson correlation function (r) between the H ($\mathrm{r}_{\mathrm{BETWEEN\text{-}ARM}}$) (Frere and Hug 2012; Tropea et al. 2013).

To obtain a reference value for evaluating these similarity indexes between sides ($\mathrm{DOT}_{-\mathrm{BETWEEN\text{-}ARM}}$ and $r_{\mathrm{BETWEEN\text{-}ARM}}$), for each task, the weight and the activation coefficients of each arm of each control subject were compared with the corresponding coefficients of the same arm of all the other controls and then were averaged across subjects and arms ($\mathrm{DOT}_{\mathrm{INTRA\text{-}ARM}}$ and $r_{\mathrm{INTRA\text{-}ARM}}$) (Pellegrino et al. 2018). To evaluate the effect of task and directions on the coefficients' activation profiles (i.e., H), we calculated their root mean square value (RMSsyn) for each direction and task (Coscia et al. 2014).

Finally, we extracted and analyzed as previously described also the muscle synergies considering only the time interval of the steady-state force production (IF steady-state). In other words, we investigated muscle synergies when the R and L arm maintained the same level of force. We considered EMG activity when the cursor reached the target and stayed inside it for 5 s. Here, the final steady-state forces must be similar, for both limbs and for all healthy participants, to reach a target in isometric conditions.

Statistical analysis

To test if the indicators related to behavioral performance, the number of synergies, and the similarity measures of muscle synergies (i.e., $\mathrm{DOT}_{\mathrm{BETWEEN\text{-}ARM}}$ and $r_{\mathrm{BETWEEN\text{-}ARM}}$) revealed differences between right and left arms and depended on the proposed task, we ran a repeated-measures ANOVA with two within-subjects' factors: "arm" and "task". The factor arm had two levels: 'R' and 'L' arm for

the performance indicators and for the number of muscle synergies; 'BETWEEN-ARM' and 'INTRA-ARM' for the similarity measures DOT and r. The factor task had 4 levels: FS, AF, RF and IF.

For the root mean square of the muscle activation patterns (RMS), the shape of the resampled normalized EMG envelopes ($r_{\text{EMG-BETWEEN-ARMS}}$) and the root mean square of the activation synergies (RMS_{syn}) we added "target direction" as another within-subjects' factor.

Post-hoc analysis (Tukey's HSD test) was performed to further investigate statistically significant main effects and interactions. As for the arm × task effect, we were interested in verifying how the different environments affected the differences between sides. We computed the difference of the indicators obtained for the left and right arms in each task and we compared this difference for each pair of tasks. Bonferroni correction for multiple comparisons was applied and Bonferroni corrected p values are reported in the text. Effects were considered significant at the $p < 0.05$ level.

The assumption of sphericity was tested on each variable using Mauchly's test. When the assumption was rejected the Greenhouse–Geisser correction was applied. The statistical analysis was computed within Statsoft environment (Statistica software 7.1, Statsoft TULSA, USA).

Results

Accuracy as kinematic marker of laterality

Movement speed, accuracy and smoothness were computed to identify which kinematic features reflected neural control of the two arms in our right-handed subjects (see "Materials and methods" section for more details). The two arms differed in terms of accuracy of the cursor trajectory in all tasks (selected subject in Fig. 2).

The L arm had larger errors (arm effect: aspect ratio: $F(1,40) = 16.29$, $p < 0.001$, Fig. 3a) with respect to the R arm. In particular, the higher aiming errors in L arm respect to the R arm also suggested differences in the feedforward control (100-ms aiming error: $F(1,40) = 27.70$, $p < 0.001$, Fig. 3c). The L arm did not completely compensate for these initial errors since they remained higher in the final part of the trajectory (end-point error: $F(1,40) = 9.40$, $p = 0.004$, Fig. 3b). Post-hoc analysis confirmed that these significant differences between R and L arms were observable in all tasks (Fig. 3a, c: aspect ratio—FS: $p = 0.03$, AF: $p = 0.03$, RF: $p < 0.001$, IF: $p < 0.001$; 100-ms aiming error—FS: $p < 0.001$, AF: $p = 0.01$, RF: $p < 0.001$, IF: $p < 0.001$; end-point error—FS: $p = 0.02$, AF: $p = 0.02$, RF: $p = 0.001$, IF: $p < 0.001$). While movements executed with the R arm were more accurate than those executed with the L arm in all tasks,

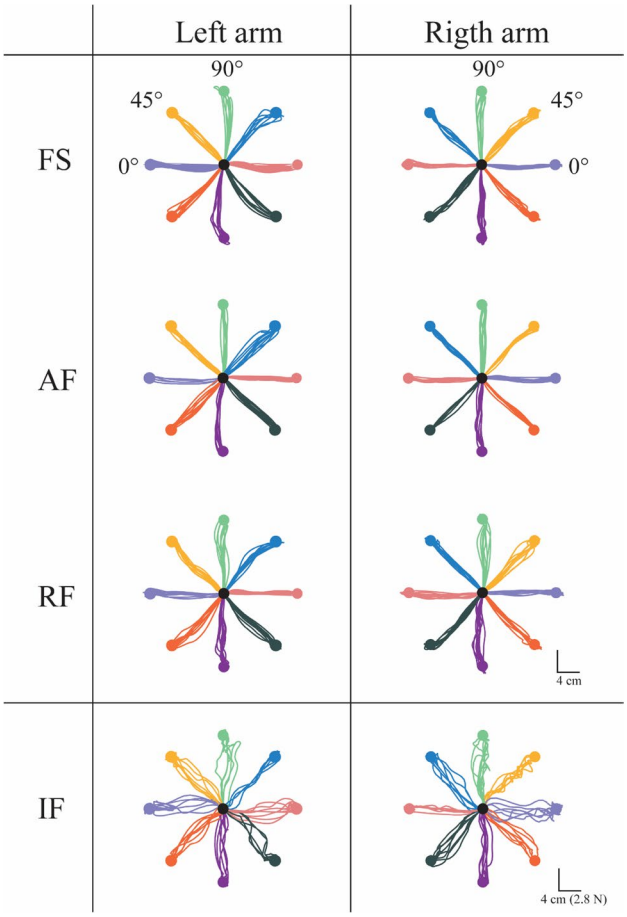

Fig. 2 Example of cursor trajectories (subject 1) for the left (first column) and the right (second column) arm in the different mechanical environments: free space (FS, first row), assistive force (AF, second row), resistive force (RF, third row) and isometric force (IF, fourth column). Equal colors correspond to equivalent movements in joint space

the difference between the two arms in terms of accuracy depended on the task (interaction effect: arm × task: end-point error: $F(3120) = 20.70$, $p = 0.001$; 100-ms aiming-error: $F(3,120) = 14.49$, $p = 0.005$; aspect ratio: $F(3,120) = 190.67$, $p < 0.001$; see, Fig. 3a, c). Subjects had more difficulty in controlling a force trajectory (IF) than a movement trajectory in free space and in presence of resistive or assistive force, i.e., they had worse performance during the isometric task than in the dynamic tasks; see Fig. 3. Specifically, the difference between sides increased in the IF task with respect to the FS, RF, and AF tasks for the 100-ms aiming error (post hoc: $p = 0.02$, $p = 0.01$ and $p = 0.02$, respectively), the aspect ratio (post hoc: $p < 0.001$ for all conditions) and the end-point error (post hoc: $p < 0.001$ for all conditions), Fig. 3a–c. Instead, as expected, the difference in accuracy between arms in the second part of the trajectory was lower in the AF task, i.e., subjects had greater end-point error in IF, FS and RF tasks

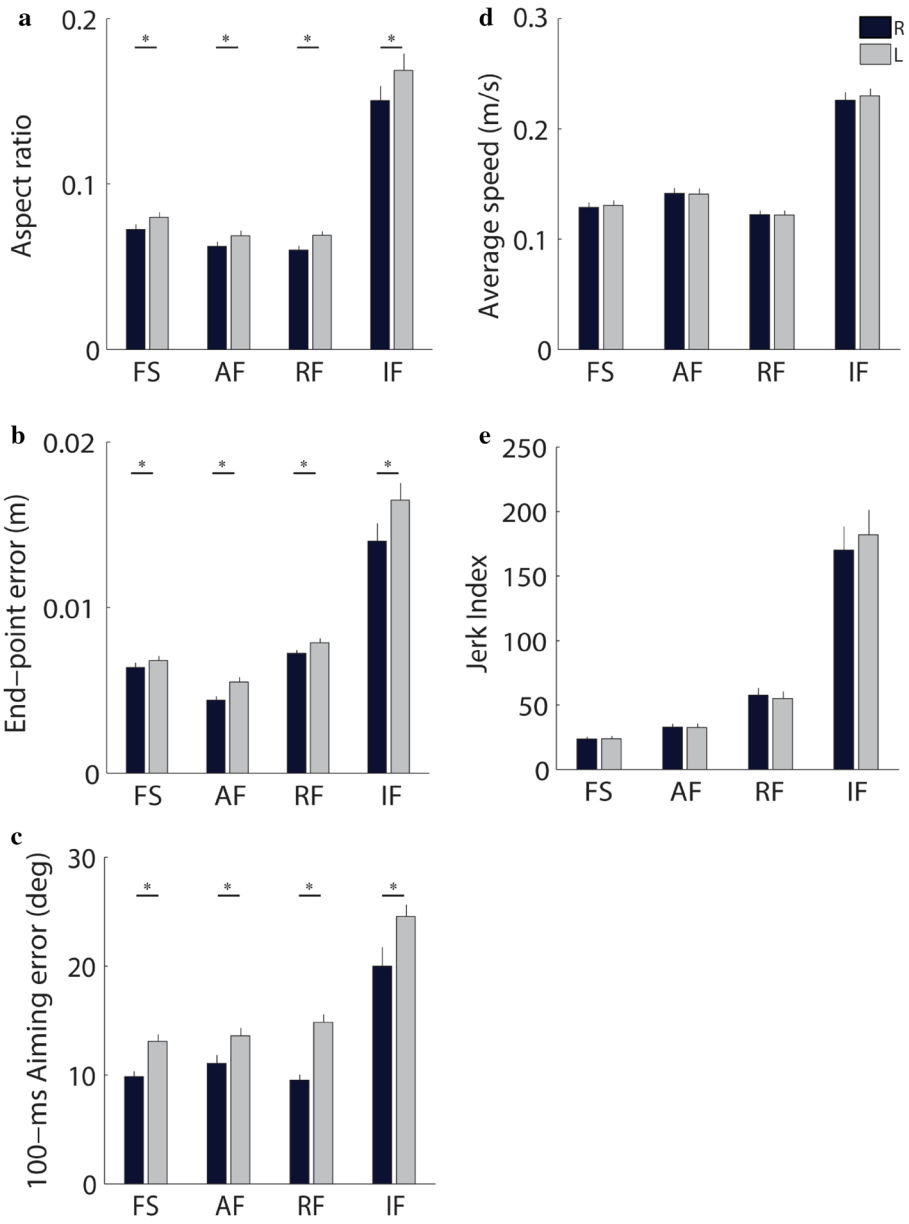

Fig. 3 Behavioral parameters related to the cursor trajectories during the free space (FS), assistive force (AF), resistive force (RF) and isometric force (IF). The height of the black and grey bars represents the mean value of the indicators for right (R) and left (L) arm, respectively; the error bars correspond to the standard error across subjects. *indicates significant ($p < 0.05$) differences between R and L arm

with respect to the AF task (post hoc: FS vs AF: $p = 0.003$; IF vs AF: $p = 0.001$ and RF vs AF: $p = 0.002$; Fig. 3b). In the initial part of the trajectory the difference in accuracy between arms was evident in the RF with respect to FS (post hoc: 100-ms aiming error: $p = 0.02$; Fig. 3c).

We did not find significant differences between arms in terms of average speed (arm effect: $F(1,40) = 2.45$, $p = 0.50$, arm × task effect: $F(3,120) = 1.75$, $p = 0.57$; Fig. 3d) and smoothness (arm effect: $F(1,10) = 1.45$, $p = 0.49$, arm × task effect: $F(3,120) = 2.43$, $p = 0.78$; Fig. 3e). Finally, as expected, during the steady-state phase of the IF task the two hands had equal performance, i.e., they exerted the same force (L arm: 10.285 ± 0.157 N and R arm: 10.214 ± 0.166 N; arm effect: $F(1,40) = 1.52$, $p = 0.847$).

Muscle synergies

The dimensionality of muscle synergies is preserved between sides

The number of muscle synergies of the R and the L arm was the same for each task (arm effect: $F(1,40) = 1.54$, $p = 0.541$); see, Fig. 4. We extracted five muscle synergies in both arms

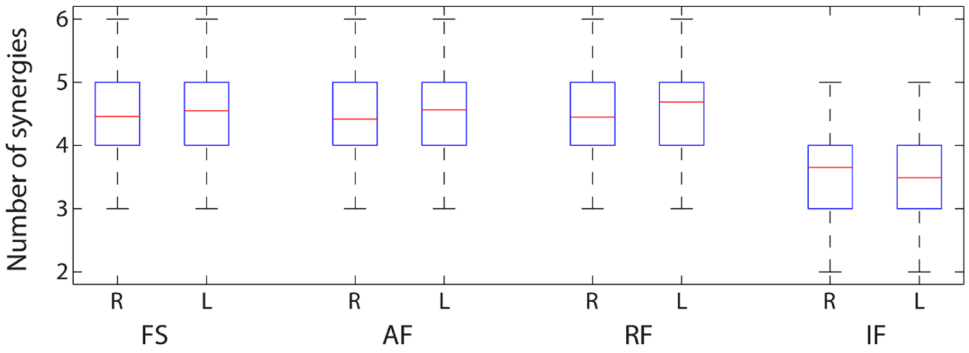

Fig. 4 Number of synergies for the different mechanical environments: free space (FS), assistive force (AF), resistive force (RF) and isometric force (IF). The red lines represent the median value computed across subjects of the number of synergies for the right (R) and the left (L) arm, and the bottom and top edges of the boxes indicate the 25th and 75th percentiles, respectively. The whiskers extend to the most extreme data points

for FS, AF, and RF tasks (Fig. 4). Instead, we found four muscle synergies in the IF task (Fig. 4). The difference in the number of muscle synergies between the isometric force task and the dynamic tasks was significant (arm × task effect: $F(3,120) = 15.82$, $p = 0.001$; post-doc: FS vs IF, AF vs IF and RF vs IF: $p < 0.001$ for both L and R; Fig. 4).

Overall muscle synergies have the same structure in the right and left arm

In the movement tasks (i.e., FS, AF and RF), the organization of the five muscle synergies had the following characteristics (Fig. 5a):

- Synergy 1 principally involved the TB-long and TB-lat.
- Synergy 2 principally involved the DELT-ant and DELT-mid, with minor contributions from other muscles. Among these, the BRA and the INFR contribution became higher and relevant in the IF task.
- Synergy 3 principally involved the DELT-post, RHOM and INFR.
- Synergy 4 principally involved the TRAP, with minor contributions from other muscles. Among these, the PECT contribution became higher and relevant in the IF task.
- Synergy 5 principally involved the BB-long, BB-short and PECT.

In the IF task, synergy 5 was absent and the contribution of the BB-long and BB-short was distributed in the other synergies; while the activity of PECT muscle was presented in synergy 4.

In all tasks, there was not a significant difference on the structure of muscle synergies of the two arms, as described by the weight coefficients, i.e., we did not find a difference ($F(1,40) = 2.12$, $p = 0.821$) between the two sides ($DOT_{BETWEEN\text{-}ARM}$), that exceeded the variability observed within sides ($DOT_{INTRA\text{-}ARM}$, see "Materials and methods" section; Fig. 5b).

The similarity between the organization of the muscle synergies between-arm and intra-arm was task-dependent (task effect: $F(3,120) = 43.71$, $p < 0.001$, Fig. 5b).

Two muscle synergies show different direction-dependent activations between sides

In both sides, the activation profile (H) of each synergy was modulated across directions so that each synergy's engagement was specific to one or two consecutive directions and the activations of the whole set of muscle synergies allowed for covering of all the workspace (Fig. 6a). The activations of synergy 2 and synergy 4 were different in the R and the L arm for all tasks, except for the AF task. These differences increased in the isometric force task.

The activation profiles of the five muscle synergies (H1-H5) had the following characteristics (Fig. 6a, b):

- H1: Synergy 1, including the activity of muscles controlling the upper arm during elbow extension for both arms, was mainly active during movements/force exertion directed toward 90° and 135° (90° and 45° for the assistive force).
- H2: Synergy 2, including the activity of muscles controlling the upper arm during horizontal shoulder abduction and extension, was mainly active during movements directed toward 90° and 135° for the L arm, and toward 45° and 90° for the R arm. In the isometric task the synergy 2 was mainly active for forces exerted toward 180° and 45°/225° for the L arm, with mirror symmetric activations for the R arm, i.e., towards 0° and 135°/315°.
- H3: Synergy 3, including the activity of muscles controlling the upper arm during horizontal shoulder adduction

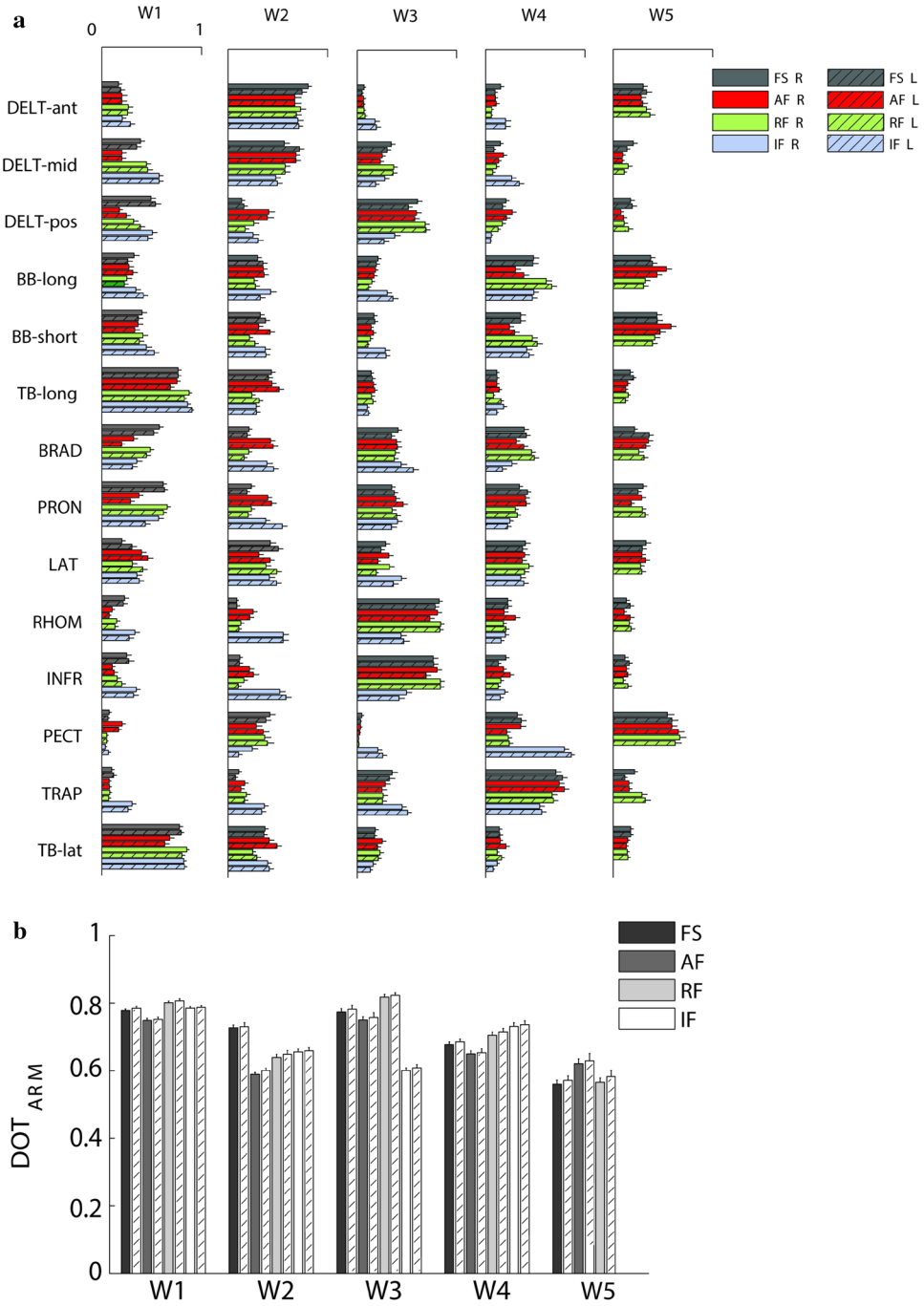

Fig. 5 **a** Weight coefficients for all muscle synergies (W1–W5) for the two arms (right, bars with uniform color and left, bars with diagonal lines). Tasks performed in different environments are shown with different colors as indicated in the legend: free space (FS, grey color), assistive force (AF, red color), resistive force (RF, green color) and isometric force (IF, blue color). Data are referred to the following muscles: Triceps Brachii long head (TB-long), Triceps Brachii lateral head (TB-lat), Biceps Brachii short head (BB-short), Biceps Brachii long head (BB-long), Brachioradialis (BRAD), Pronator Teres (PRON), Infraspinatus (INFR), Latissimus dorsi (LAT), Upper Trapezius (TRAP), Rhomboid Major (RHOM), Pectoralis Major (PECT), Anterior Deltoid (DELT-ant), Medial Deltoid (DELT-mid) and Posterior Deltoid (DELT-post). The error bars represent the standard error. **b** Comparison between arms of weight coefficients of the muscle synergies by the scalar product (DOT). Bars with uniform colors indicate the DOT values obtained by comparing the weight coefficients of R vs L arm ($DOT_{BETWEEN\text{-}ARM}$) across subjects, for each synergy, W1–W5, and each task (back to white colors). The bar streaked in black indicates the corresponding values obtained comparing across subjects the weight coefficients of a same arm. The two DOT values computed separately for the R and L arm were averaged to obtain the $DOT_{INTRA\text{-}ARM}$ reported in the figure. The error bars correspond to the standard error

and flexion, was mainly active during movements/force exertion directed toward 0°, 270° and 315°.

- H4: Synergy 4, including the activity of muscles controlling the elevation of the shoulder, was active during movements directed toward 270° and mainly toward 225° for the R arm, 315° for the L arm. In the isometric task, the synergy 4 was mainly active for forces exerted towards 180° and 45°/225° for the R arm, with mirror symmetric activations for the L arm, i.e., towards 0° and 135°/315°.
- H5: Synergy 5, including the activity of muscles controlling the upper arm during elbow flexion and the shoulder adduction, was mainly active (H5) during movements directed toward 180° and 225°.

We found a significant difference between the two arms in the activation profiles, (i.e., $r_{BETWEEN\text{-}ARM}$ vs $r_{INTRA\text{-}ARM}$: $F(1,40) = 89.0$, $p < 0.001$, Fig. 6c) and this difference was also synergy and task dependent (interaction effect—arm× task× synergies: $F(9,360) = 12.97$,

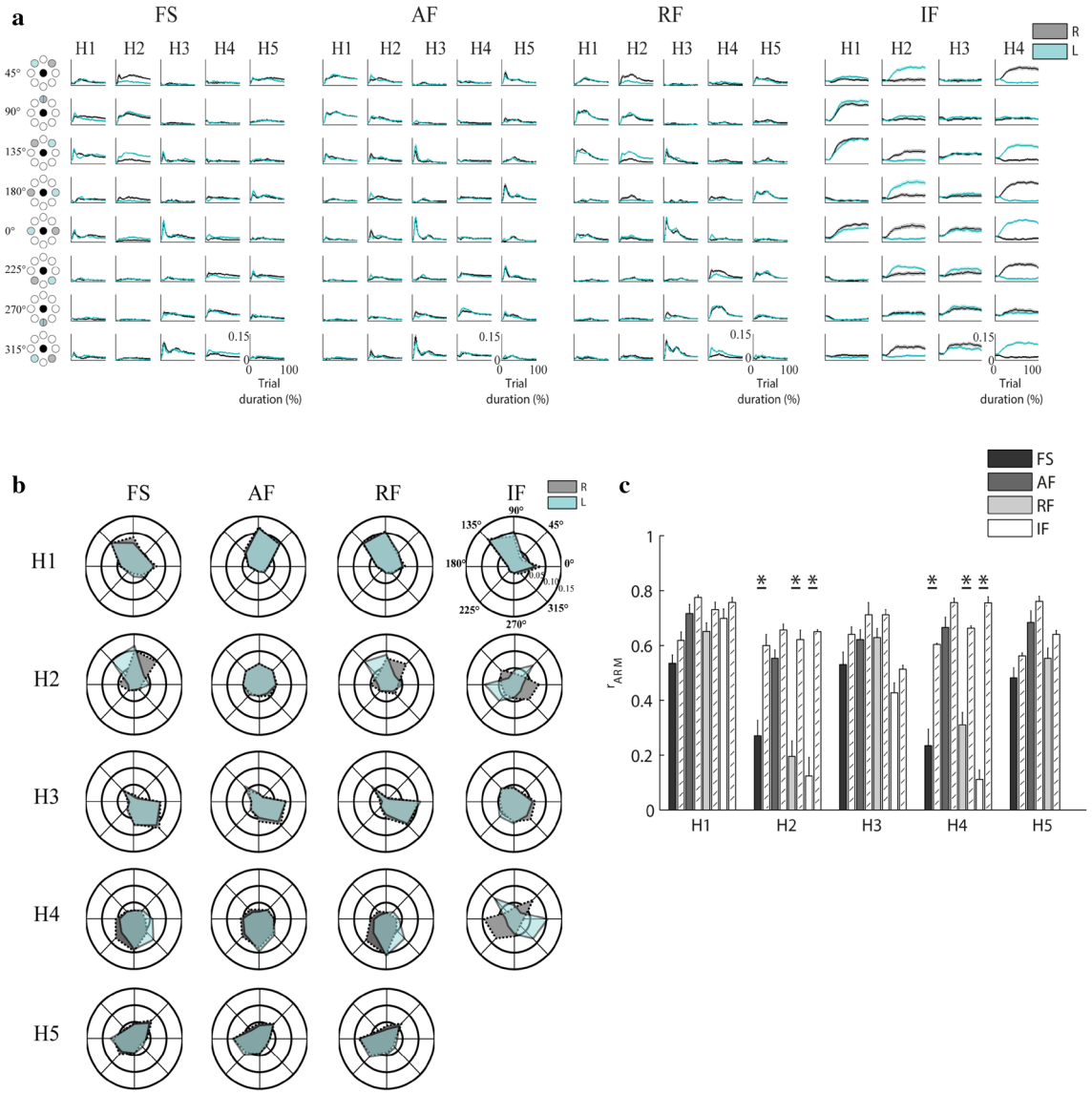

Fig. 6 **a** Activation profile coefficients of the muscle synergies (H1–H5) for the two arms [grey: right (R) and cyan: left (L)] in FS (free space, first column), AF (assistive force, second column), RF (resistive force, third column) and IF (isometric force, fourth column) task. The shaded area corresponds to the standard error. **b** Polar plots of mean RMS for the activation profiles coefficients of the muscle synergies (H1–H5) in FS (free space, first column), AF (assistive force, second column), RF (resistive force, third column) and IF (isometric force, fourth column). Each radial line represents one of eight directions. For each direction, mean RMS of the activation profiles coefficients for right (R, grey) and left (L, cyan) arm, respectively. For **a** and **b**, right and left activation profile coefficients of the muscle synergies are referred to equal movements in the joint space; i.e., for each column the left panel indicates the corresponding target directions (grey target) for the R arm, while the corresponding target directions of the L arm were mirror symmetric with respect to the vertical midline (cyan target). **c** Comparison of the activation profile coefficients of the muscle synergies between R and L arm by Pearson correlation (r). Bars with uniform colors indicate the r values obtained by comparing the activations coefficients of R vs L arm ($r_{\text{BETWEEN-ARM}}$) across subjects, for each synergy, H1–H5, and each task (black to white colors). The bar streaked in black for indicate the corresponding values obtained by comparing across subjects the activation profiles of a same arm. The two r-values computed for the R and L arm were averaged to obtain the $r_{\text{INTRA-ARM}}$ reported in the figure. The error bars correspond to the standard error. *indicates significant differences ($p < 0.05$) between $r_{\text{BETWEEN-ARM}}$ and the $r_{\text{INTRA-ARM}}$

$p < 0.0001$). Specifically, the activation profiles H2 and H4 were different between sides during the FS, RF and IF tasks ($p < 0.001$ in all conditions), but not during the AF task.

Similarly, the RMS activation profiles (RMS_{syn}, Fig. 6b) were significantly different between the two sides (arm effect: $F(1,40) = p < 0.001$; interaction effects: arm× task× synergies: $F(9,360) = 111.26$, $p < 0.001$;

arm× task× synergies× direction: $F(9,360) = 56.32$, $p < 0.001$); Specifically, H2 and H4 were different in all tasks except for AF (post hoc—FS: $p \leq 0.002$, RF: $p = 0.001$, IF ≤ 0.001; AF $= p > 0.4$ for both H2 and H4). Instead we did not find significant differences between arms for the RMS of H1, H3 and H5 ($p > 0.10$).

In summary, RMS_{syn} and $r_{BETWEEN\text{-}ARM}$ revealed a different direction-dependent activation of synergies 2 and 4 for the two arms. From the starting position on the body midline, the R arm reached the ipsilateral targets (i.e., targets on the right workspace) mainly activating synergies 2 and 3, and the contralateral targets (i.e., the targets on left workspace) activating synergies 1, 4 and 5, while the L arm reached the ipsilateral targets (i.e., the targets on left workspace) mainly activating synergies 4 and 3, and the contralateral targets (i.e., the targets on the right workspace) mainly activating synergies 1, 2 and 5. For the task IF, the opposite behavior of H2 and H4 for the two arms was more marked: in the right arm, H2 was active for the ipsilateral targets and H4 for the contralateral targets, while in the left arm, H4 was active for the ipsilateral targets and H2 for the contralateral targets.

During IF steady-state, the number of muscle synergies was the same for R and L arm and the same of the IF task. We extracted four muscle synergies in both arms and the number of synergies was not significantly different between arms ($F(1,40) = 1.77$, $p = 0.34$). The organization and the activation of the four muscle synergies was similar to the ones in IF task (Figs. S2 and S3 panel A). There was not a significant difference in the structure of muscle synergies of the two arms, as described by the weight coefficients, i.e., we did not find a difference between $DOT_{BETWEEN\text{-}ARM}$ and $DOT_{INTRA\text{-}ARM}$, ($F(1,40) = 3.22$, $p = 0.901$); see, Fig. S2. We found a significant difference between the two arms in the activation profiles, (i.e., $r_{BETWEEN\text{-}ARM}$ vs $r_{INTRA\text{-}ARM}$: $F(1,40) = 91.05$, $p < 0.001$, Figure S3) and this difference was synergy dependent (interaction effect − arm× synergies: $F(3,120) = 42.15 p < 0.0001$); see Fig. S3. Specifically, the activation profiles H2 and H4 were different between sides with respect to H1 and H3 ($p < 0.001$); Fig. S3 panel C. Finally, the RMS activation profiles (RMS_{syn}, Fig. S3 panel B) were significantly different between the two sides (arm effect: $F(1,40) = 22.54$, $p < 0.001$; interaction effects: arm× synergies: $F(3,120) = 42.60$, $p < 0.001$; arm× synergies× direction: $F(3,360) = 48.47$, $p < 0.001$). Instead we did not find significant differences between arms for the RMS of H1, H3 and H5 ($p > 0.21$); see, Fig. S3 panel B.

In summary, even focusing in the steady-state in IF task, when task execution is more similar, RMS_{syn} and $r_{BETWEEN\text{-}ARM}$ revealed a different direction-dependent activation of synergies 2 and 4 for the two arms, as in IF condition.

EMG analysis revealed which muscles had the most influence on the different activation profiles between sides

The activation profile of single-muscle activity differed between the R and L arm (Fig. 6a) for the FS, RF and the IF task, but not for the AF task, and this difference was direction-dependent (i.e., comparing $r_{EMG\text{-}BETWEEN\text{-}ARM}$ vs $r_{EMG\text{-}INTRA\text{-}ARM}$:,—arm effect $F(1,40) = 90.47$, $p < 0.001$; arm× task effect: $F(3,240) = 68.43$, $p < 0.001$, post hoc FS: $p = 0.010$, RF: $p = 0.001$, IF: $p < 0.001$ AF: $p = 0.249$; arm × task × direction effect: $F(5,240) = 52.41$, $p < 0.001$). However, the differences between sides in the modulation

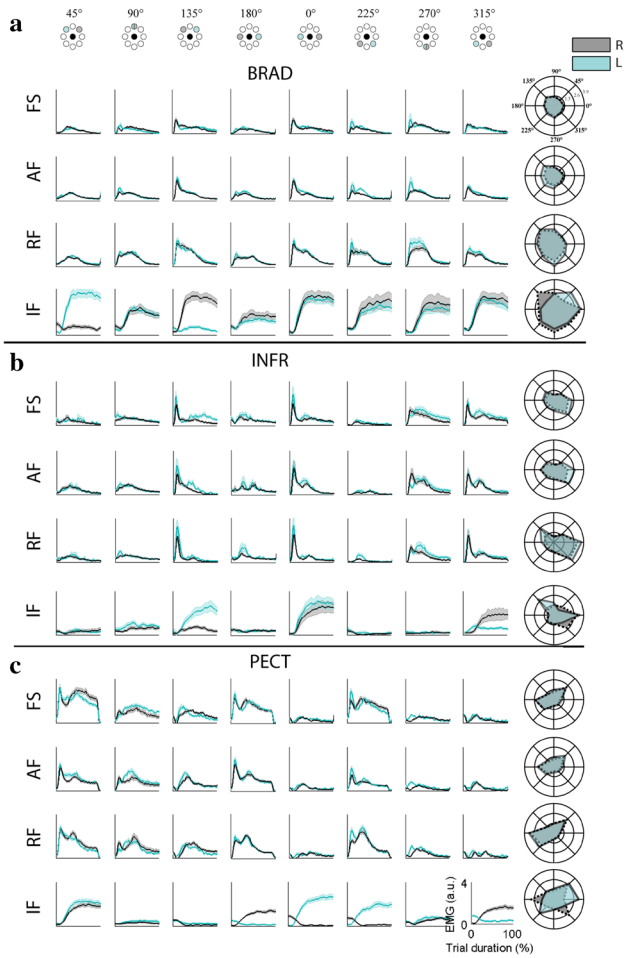

Fig. 7 Envelopes of the EMG activity and polar plots of mean RMS of the muscle activation for brachioradialis (**a**, BRAD), infraspinatus (**b**, INFR) and pectoralis major (**c**, PECT) during reaching movements for the eight target directions (top panel) in free space (first row, FS), assistive force (second row, AF), resistive force (third row, RF) and isometric force (fourth row, IF) tasks. The grey and cyan profiles represent the muscle activation for right (R) and left (L) arm, respectively. Muscle signals of R and L arm are referred to equal movements in the joint space; i.e., for each column the top panel indicates the corresponding target directions (grey target) for the R arm, while the corresponding target directions of the L arm were mirror symmetric with respect to the vertical midline (cyan target)

of the activation across directions of each single muscle became evident in the IF task, while they were small and difficult to detect in the dynamic tasks. For example, in the R arm the BRAD had higher activations in the 135° than in 45° direction, while in the L arm had the opposite behavior (i.e., higher activations in the 45° than in the 135° direction). The INFR had the higher activations in the 0° and 315° directions in the R arm, and in the 0° and 135° directions for the L arm. The PEC had the higher activations in the 45°, 180°, 315° directions in the R arm, and in the 0°, 45°, 225° directions in the L arm.

The different modulation in the IF task of BRAD and INFR activations agrees with the different activation between sides of synergy 2 (Figs. 6a and 7a, b), while the different modulation of PECT activation agrees with the different activation of synergy 4 (Figs. 6a and 7c). Conversely in the dynamic tasks where muscle activations had less marked differences between the two arms, the behavior of the activation of synergy 2 and 4 was less evident.

Discussion and conclusions

The main finding of the present study is that muscles synergies extracted from multiple EMG signals have different activations for the two arms of right-handed individuals. This result supports our hypothesis that, muscle synergies extracted from the factorization of EMG signals can reflect neural control, when the tasks and the biomechanical constraints are taken into proper account in the experimental design.

Specifically, in our experiment two muscle synergies (S2 and S4) were activated in a different direction-dependent manner between the two body sides for the medio-lateral directions, in three out of the four tasks, and in particular in the IF task. These two synergies had complementary roles in the two sides: ipsilateral targets were reached with the activation of S2 in the R arm and S4 in the L arm; contralateral targets were reached with the activation of S4 for the R arm, and S2 for the L arm. Synergies 1, 3, 5 had similar activations between sides.

These results support the conclusion that synergies are not only a mere by-product of biomechanical or task constraints, but they are also a consequence of neural information processing (Hart and Giszter 2010; Yakovenko et al. 2011; Overduin et al. 2012; Bizzi and Cheung 2013). According to this theory, the cortex selects, combines and modulates the appropriate spinal inter-neuronal modules (described by the weight coefficients) with temporal patterns of activation (described by the activation profile coefficients) that are necessary to perform a specific motor task (Bizzi and Cheung 2013). The difference between sides in the activation of muscle synergies (H2 and H4) extracted from the factorization of EMG signals provides evidence that in right-dominant adults the CNS activates different motor commands to control muscle coordination for the left and right arms, with consequent differences in movement execution, and accuracy.

The direction-dependent control of the activation of muscle synergies is also in agreement with the findings of D'Avella (d'Avella et al. 2008) demonstrating that synergies are activated in preferred directions and behave as different cosine functions with different onset times. Moreover, the robustness in the composition of muscle synergies across subjects and sides as well as the consistency with other studies, further reinforces the hypothesis that muscle synergies obtained from the factorization of EMG signals are actual coordination patterns common to individuals and tasks (d'Avella et al. 2006; Latash and Anson 2006; d'Avella et al. 2011) influenced by neural control. Unfortunately, our experimental data allowed for confirming the influence of neural control in muscle synergies, but does not explain how the observed differences between the muscle synergies activations were originated.

We could not observe the influence of neural control in the number and organization (weight coefficients) of the muscle synergies. Given the difference in motor performance between sides, we could have expected that the dimensionality of muscle synergies could have been directly influenced, as it was found in a small group of subjects during the execution of fine movements (Duthilleul et al. 2015). However, previous findings on stroke survivors (Cheung et al. 2009b, 2012) indicated that during reaching movements significant differences in the structure of the muscle synergies appeared only when the performance was highly degraded, but not in the presence of mild-to-moderate loss of motor abilities. Therefore, we can hypothesize that a structural difference in the muscle synergies might arise in precision tasks, but not in planar reaching movements. As for the weight coefficients, they were similar to those already reported in other studies (d'Avella et al. 2006; Roh et al. 2013; Tropea et al. 2013) for both the R and the L arm. The general preservation of the weight coefficients between sides in each task is supportive of the hypothesis that the weights of muscle synergies are the fixed components of the neural signals, the building blocks that are combined to achieve different tasks. The robustness of the muscle synergies across arms suggests that these synergies are structured most likely by neuronal networks downstream of the neocortex, such as the spinal interneuronal circuitries and/or neurons in the brainstem nuclei as suggested by Cheung et al. (2009b). According to this view, movement is generated through a combination of modules organized within the spinal cord (Cheung et al. 2009b; Bizzi and Cheung 2013). However, we cannot exclude the possibility of muscle-specific differences in the composition of the weight coefficients between

sides since we did not investigate if there were differences between sides in the contribution of each muscle to the weight coefficients because of the high complexity of the analysis for excessive multiple comparisons (muscles, synergies, tasks, directions and sides). In summary, our results provide experimental evidences of the influence of neural control on muscle synergy activation patterns, but not on the weight coefficients during planar arm reaching tasks, and in a short time frame. In a short time frame, weight coefficients might be more dependent on factors, such as the task (Kutch and Valero-Cuevas 2011, 2012) and anatomical constraints (Neptune et al. 2009; Kutch and Valero-Cuevas 2011; Levine et al. 2014; Steele et al. 2015). Indeed, the similarity of weight coefficients between sides was task-dependent, and the difference in the activations H2 and H4 between sides was particularly strong in the IF task, while it was not observable in the presence of assistive forces. As for the anatomical constraints, we compare the two arms that have quite similar anatomical structure. Our evidence does not exclude that observation in a longer time frame, the number of muscle synergies and the weight coefficients would reveal neural control, as experimental data suggests (Dominici et al. 2011).

The results of the muscle synergy analysis were supported by the single-muscle analysis. Indeed, the main muscles participating in synergy 2 and 4 reflected as well the different motor control strategies between the two limbs in right-handed adults. However, we found remarkable differences between sides in few muscles and mainly in isometric conditions, while two out of four/five muscle synergy activations differed between sides in three out of four conditions. Therefore, muscle synergies highlighted the different control strategies between sides more than muscle activity.

Differences between the two sides of the body in the activity of specific muscles during planar reaching movements in free space and without anti-gravity support (toward two targets corresponding to our 45° and 135°) was found also by Bagesteiro and Sainburg (2002). They observed that the activity of elbow (biceps) and shoulder (pectoralis) flexors had substantially less amplitude for the right dominant arm, while the elbow and shoulder extensor did not show reliable differences in amplitude. In the present study, we compared the resampled normalized EMG envelopes between sides in term of their shape, but not as amplitude because the normalization for the median that we adopted does not allow eliminating differences between sides due to electrode placement. Moreover, we compared muscle activity of the two sides by looking at the distribution of the RMS across the different directions. The activity of the PECT was remarkably different between the two arms also in our study, but only in the IF task, while we did not observe significant differences between sides in the elbow flexors. This might be due to the arm support.

Therefore, with respect to the analysis of single-muscle activity, our findings enrich the previous literature, suggesting that upper limb muscle activity in right-handed adults might differ between sides in few muscles acting in specific directions, and the adoption of the isometric task helps to highlight this aspect.

In addition to muscle activity and synergies, our results also clarify which features of movement execution are sensitive to laterality for right-handed adults. We found that the metrics underlying accuracy were sensitive to handedness as also reported in other studies (Sainburg 2002; Sainburg and Schaefer 2004; Sainburg 2005; Wang and Sainburg 2007). The left non-dominant arm had higher errors with respect to the right dominant arm in all tasks; in particular, the behavioral performance of the isometric task provided strong evidence that the L arm was less accurate then the R arm.

Previous studies already showed that movements of the dominant hand are more accurate than those performed by the other hand during repetitive line-drawing tasks (Woodworth 1899), suggesting that movement planning is more effective and consistent for the dominant arm. Dominant arm advantages are also evident during handwriting (Blank et al. 2000) and when aiming at static targets (Sainburg 2002). Movement time tends to be shorter in the dominant arm relative to the non-dominant arm during rapid aiming movements and unimanual reaching tasks (Annett et al. 1979; Roy et al. 1994; van Doorn 2008). During time-measured aiming, reaching and pointing tasks, the dominant arm shows higher peak velocities (Annett et al. 1979; Heath and Roy 2000; Boulinguez et al. 2001), shorter movement time and better accuracy (Elliott et al. 1993), and reaction time is lower in the non-dominant arm during planar reaching movements (Carson et al. 1992; Elliott et al. 1993; Carson et al. 1995). The average speed of cursor movements remained relatively similar between the arms in our experiments, while according to the literature we would have expected also differences in speed between the two sides. Other studies, indeed, showed that movement durations were shorter in the dominant arm during rapid aiming movements (Annett et al. 1979; Roy et al. 1994; van Doorn 2008) and the reaction times were shorter in the non-dominant arm (Carson et al. 1992; Elliott et al. 1993). However, in these studies, subjects were required to perform fast movements. In our study, instead, subjects performed the reaching movements at a self-selected speed, with the goal to be as accurate as possible. Therefore, in our population of right-handed adults, the neural control might be optimized for reaching a specific goal, i.e., in our case accuracy, and consequently laterality, might affect mainly the metrics related to this goal, having lower or no effects on the other motor performance, such as speed.

Note that to deepen how handedness influences muscle synergies would require enrolling left-handed individuals.

This however, would be beyond the scope of this study. Our goal was to reveal the influence of neural control on muscle synergies extracted from EMG signals by eliminating confounding factors. Thus, we enrolled only right-handed adults, i.e., a homogeneous group of subjects whose dominant hand was primarily controlled by the left hemisphere of the brain. We focused on arm reaching movements instead of fine motor tasks to minimize the impact of minor biomechanical differences between upper limbs in favor of neural control differences that would become apparent on larger scale movements.

Finally, our results provide suggestions for clinical applications. Indeed, the analysis of the muscle activation patterns in terms of muscle synergies and behavioral performance have been proposed as a basis for the development of customized therapeutic strategies for people with reduced motor coordination, such as people affected by stroke (Cheung et al. 2009b, 2012), multiple sclerosis (Pellegrino et al. 2018) and spinal cord injury (Ting et al. 2015; Torricelli et al. 2016; Coscia et al. 2018). Our study provides sensitive markers of motor control abilities for healthy individuals, such as movement accuracy and the activations of muscle synergies, confirming their utility in quantitatively assessing motor performance and modified motor control strategies. There is evidence that abnormal kinematic synergies can be modified by targeted motor training (Dipietro et al. 2007). We observed that in healthy adults the organization of muscle synergies was preserved across tasks, but the direction-dependent modulation of muscle synergy activations might be dependent on the mechanical proprieties of the environment. It may be possible to design studies to track the changes of the abnormal muscle synergies during the recovery process, e.g., in acute stroke survivors, or as results of a rehabilitation treatment. When combined with functional brain imaging, these studies may provide new insight into the neural reorganization after brain damage and may help to define the nature and the timing of the therapeutic interventions. Further investigations with different populations suffering from neurological diseases are necessary to understand how precisely it is possible to tune muscle synergy components by modifying the mechanical proprieties of the environment. This would open the possibility to develop training protocols that focus more directly on abnormal muscle synergy structure and/or recruitment patterns.

Limitations

This work is based on the underlying assumption that our results are robust with respect to the variability of EMG signals, i.e., that any difference between sides is purely neural and not due to the variability of EMG signals. EMG signals are robust enough to identify similar and robust features across healthy individuals (Zardoshti-Kermani et al. 1995; Muceli et al. 2014; Batzianoulis et al. 2017) including muscle synergies (Roh et al. 2012; Ison and Artemiadis 2014), and to achieve sufficient accuracy for myoelectric prosthetics control (Cipriani et al. 2011), However, variability in EMG signals is unavoidable due to the intrinsic limitation of superficial surface EMG recording, for example including the not identical electrodes placements or presence of adipose tissue between the arms (Kuiken et al. 2003).

For this reason, the results were based on many subjects and we included in this work also single EMG analysis of many muscles to complement muscle synergies analysis. Moreover, we carefully verified that the difference we found between arms was above the variability of the EMG signals that affects the same measures when computed across subjects for a same side, either the left or the right arm. The same person placed the electrodes in the right and left side of all subjects following the same procedures for both arms, the same analysis was applied to all the recordings, thus the variability of the measure of EMG signals due to limitations in their recordings should be accounted in the standard deviation across individuals and the differences we found between arms were significant taking into account this inter-subjects variability. In addition to muscle activity and synergies, our results show also a difference in task execution between the right and left arm as reported by some of the metrics that we measured (aspect ratio, end-point error and 100 ms aiming error). This difference in task execution reflects different control strategies, consequent to the different neural control between sides, as previous literature on the effect on handedness on motor performance also suggested (Sainburg 2002; Sainburg and Schaefer 2004; Sainburg 2005; Wang and Sainburg 2007). While finding different activations in correspondence of different performance was expected, it was surprising that in a well-controlled task and with the difference in performance being rather small, two muscle synergies had opposite activations. Different muscle synergies when task performance is different could reveal different control strategies, but it cannot be excluded that different muscle activity and coordination can be a consequence of the different task execution. The neural origin can be attributed as the main cause of different muscle synergies and task performance in a task where the two arms have the same performance. Therefore, to further prove the neural origin of differences in muscle synergies activations, we repeated the synergies analysis considering only the steady state of the force production in the IF task. By definition of this task, the final steady-state forces have to be similar, for both limbs and for all healthy participants, to reach a target in isometric conditions. Finding in this latter case that similar limbs, produced the same forces with different muscle synergies activations provided further-convincing evidence

for our main hypothesis related to the neural origin of the muscle synergies.

Acknowledgements The authors are grateful to all participants of the study for volunteering their time. We want to thank Giorgia Stranieri, Amel Chief and Maddalena Mugnosso for the help during the experimental sessions, Dr. Susanna Summa and Dr. Camilla Pierella for helpful suggestions, Prof. Ferdinando Mussa-Ivaldi for his advice and critical review of the manuscript, Prof. Niels Birbaumer for his further revision of the manuscript, and Brenda Klem for proofreading the manuscript.

Author contributions All the authors conceived the study, designed the experimental protocol and developed the experimental setup. LP collected the data. All authors analyzed the results, contributed to the discussion of the results and to writing of the manuscript. All authors read and approved the final manuscript.

Funding This research was supported by Italian Multiple Sclerosis Foundation (FISM, 2013- Cod. 2013/R/5) and by Marie Curie Integration Grant FP7-PEOPLE- 2012-CIG- 334201 (REMAKE) Research projects of national interest (ModuLimb, PRIN-2015HFWRYY).

Data availability The data sets analyzed during the current study are available from the corresponding author upon reasonable request.

Compliance with ethical standards

Conflict of interest The authors declared no potential conflict of interest with respect to the research, authorship, and/or publication of this article.

References

Adam A, De Luca CJ, Erim Z (1998) Hand dominance and motor unit firing behavior. J Neurophysiol 80:1373–1382

Alessandro C, Delis I, Nori F, Panzeri S, Berret B (2013) Muscle synergies in neuroscience and robotics: from input-space to task-space perspectives. Frontiers in computational neuroscience 7:43

Annett M (1970) A classification of hand preference by association analysis. Br J Psychol 61:303–321

Annett M (2002) Handedness and brain asymmetry: the right shift theory. Psychology Press, Hove, East Sussex

Annett J, Annett M, Hudson P, Turner A (1979) The control of movement in the preferred and non-preferred hands. Q J Exp Psychol 31:641–652

Auerbach BM, Ruff CB (2006) Limb bone bilateral asymmetry: variability and commonality among modern humans. J Hum Evol 50:203–218

Bagesteiro LB, Sainburg RL (2002) Handedness: dominant arm advantages in control of limb dynamics. J Neurophysiol 88:2408–2421

Barroso FO, Torricelli D, Moreno JC, Taylor J, Gomez-Soriano J, Bravo-Esteban E, Piazza S, Santos C, Pons JL (2014) Shared muscle synergies in human walking and cycling. J Neurophysiol 112:1984–1998

Batzianoulis I, El-Khoury S, Pirondini E, Coscia M, Micera S, Billard A (2017) EMG-based decoding of grasp gestures in reaching-to-grasping motions. Robot Auton Syst 91:59–70

Berger DJ, d'Avella A (2014) Effective force control by muscle synergies. Front Comput Neurosci 8:46

Bernstein N (1967) The co-ordination and regulation of movements. Pergamon Press, Oxford

Bizzi E, Cheung VC (2013) The neural origin of muscle synergies. Front Comput Neurosci 7:51

Blank R, Miller V, von Voss H (2000) Human motor development and hand laterality: a kinematic analysis of drawing movements. Neurosci Lett 295:89–92

Boulinguez P, Nougier V, Velay JL (2001) Manual asymmetries in reaching movement control. I: study of right-handers. Cortex J Devot Study Nerv Syst Behav 37:101–122

Cappellini G, Ivanenko YP, Poppele RE, Lacquaniti F (2006) Motor patterns in human walking and running. J Neurophysiol 95:3426–3437

Carson RG, Goodman D, Elliott D (1992) Asymmetries in the discrete and pseudocontinuous regulation of visually guided reaching. Brain Cogn 18:169–191

Carson RG, Chua R, Goodman D, Byblow WD, Elliott D (1995) The preparation of aiming movements. Brain Cogn 28:133–154

Casadio M, Sanguineti V, Morasso PG, Arrichiello V (2006) Braccio di Ferro: a new haptic workstation for neuromotor rehabilitation. Technol Health Care 14:123–142

Casadio M, Sanguineti V, Solaro C, Morasso PG (2007) A haptic robot reveals the adaptation capability of individuals with multiple sclerosis. Int J Robot Res 26:1225–1233

Casadio M, Sanguineti V, Morasso P, Solaro C (2008) Abnormal sensorimotor control, but intact force field adaptation, in multiple sclerosis subjects with no clinical disability. Mult Scler 14:330–342

Cheung VC, d'Avella A, Tresch MC, Bizzi E (2005) Central and sensory contributions to the activation and organization of muscle synergies during natural motor behaviors. J Neurosci 25:6419–6434

Cheung VC, d'Avella A, Bizzi E (2009a) Adjustments of motor pattern for load compensation via modulated activations of muscle synergies during natural behaviors. J Neurophysiol 101:1235–1257

Cheung VC, Piron L, Agostini M, Silvoni S, Turolla A, Bizzi E (2009b) Stability of muscle synergies for voluntary actions after cortical stroke in humans. Proc Natl Acad Sci USA 106:19563–19568

Cheung VC, Turolla A, Agostini M, Silvoni S, Bennis C, Kasi P, Paganoni S, Bonato P, Bizzi E (2012) Muscle synergy patterns as physiological markers of motor cortical damage. Proc Natl Acad Sci 109:14652–14656

Cipriani C, Antfolk C, Controzzi M, Lundborg G, Rosen B, Carrozza MC, Sebelius F (2011) Online myoelectric control of a dexterous hand prosthesis by transradial amputees. IEEE Trans Neural Syst Rehabilit Eng 19:260–270

Corballis MC (1983) Human laterality. Academic Press, New York

Coscia M, Cheung VC, Tropea P, Koenig A, Monaco V, Bennis C, Micera S, Bonato P (2014) The effect of arm weight support on upper limb muscle synergies during reaching movements. J Neuroeng Rehabilit 11:22

Coscia M, Monaco V, Martelloni C, Rossi B, Chisari C, Micera S (2015) Muscle synergies and spinal maps are sensitive to the asymmetry induced by a unilateral stroke. J Neuroeng Rehabilit 12:39

Coscia M, Tropea P, Monaco V, Micera S (2018) Muscle synergies approach and perspective on application to robot-assisted rehabilitation. In: Rehabilitation Robotics, Elsevier, pp 319–331

Danziger Z, Mussa-Ivaldi FA (2012) The influence of visual motion on motor learning. J Neurosci 32:9859–9869

d'Avella A, Saltiel P, Bizzi E (2003) Combinations of muscle synergies in the construction of a natural motor behavior. Nat Neurosci 6:300–308

d'Avella A, Portone A, Fernandez L, Lacquaniti F (2006) Control of fast-reaching movements by muscle synergy combinations. J Neurosci 26:7791–7810

d'Avella A, Fernandez L, Portone A, Lacquaniti F (2008) Modulation of phasic and tonic muscle synergies with reaching direction and speed. J Neurophysiol 100:1433–1454

d'Avella A, Portone A, Lacquaniti F (2011) Superposition and modulation of muscle synergies for reaching in response to a change in target location. J Neurophysiol 106:2796–2812

Diederichsen LP, Norregaard J, Dyhre-Poulsen P, Winther A, Tufekovic G, Bandholm T, Rasmussen LR, Krogsgaard M (2007) The effect of handedness on electromyographic activity of human shoulder muscles during movement. J Electromyogr Kinesiol 17:410–419

Dipietro L, Krebs HI, Fasoli SE, Volpe BT, Stein J, Bever C, Hogan N (2007) Changing motor synergies in chronic stroke. J Neurophysiol 98:757–768

Dominici N, Ivanenko YP, Cappellini G, d'Avella A, Mondì V, Cicchese M, Fabiano A, Silei T, Di Paolo A, Giannini C (2011) Locomotor primitives in newborn babies and their development. Science 334:997–999

Duthilleul N, Pirondini E, Coscia M, Micera S (2015) Effect of handedness on muscle synergies during upper limb planar movements. Conf Proc Ann Int Conf IEEE Eng Med Biol Soc IEEE Eng Med Biol Soc Ann Conf 2015:3452–3455

Elliott D, Roy EA, Goodman D, Carson RG, Chua R, Maraj BK (1993) Asymmetries in the preparation and control of manual aiming movements. Can J Exp Psychol Revue 47:570

Farina D, Kallenberg LA, Merletti R, Hermens HJ (2003) Effect of side dominance on myoelectric manifestations of muscle fatigue in the human upper trapezius muscle. Eur J Appl Physiol 90:480–488

Flanders M (1991) Temporal patterns of muscle activation for arm movements in three-dimensional space. J Neurosci 11:2680–2693

Freitas SM, Duarte M, Latash ML (2006) Two kinematic synergies in voluntary whole-body movements during standing. J Neurophysiol 95:636–645

Frere J, Hug F (2012) Between-subject variability of muscle synergies during a complex motor skill. Front Comput Neurosci 6:99

Friedli WG, Fuhr P, Wiget W (1987) Detection threshold for percutaneous electrical stimuli: asymmetry with respect to handedness. J Neurol Neurosurg Psychiatry 50:870–876

Fugl-Meyer A, Eriksson A, Sjöström M, Söderström G (1982) Is muscle structure influenced by genetical or functional factors? A study of three forearm muscles. Acta Physiol 114:277–281

Giszter S, Patil V, Hart C (2007) Primitives, premotor drives, and pattern generation: a combined computational and neuroethological perspective. Prog Brain Res 165:323–346

Goble DJ, Brown SH (2008) The biological and behavioral basis of upper limb asymmetries in sensorimotor performance. Neurosci Biobehav Rev 32:598–610

Hart CB, Giszter SF (2010) A neural basis for motor primitives in the spinal cord. J Neurosci 30:1322–1336

Heath M, Roy EA (2000) The expression of manual asymmetries following extensive training of the nondominant hand: a kinematic perspective. Brain Cogn 43:252–257

Hermens HJ, Freriks B, Disselhorst-Klug C, Rau G (2000) Development of recommendations for SEMG sensors and sensor placement procedures. J Electromyogr Kinesiol 10:361–374

Ison M, Artemiadis P (2014) The role of muscle synergies in myoelectric control: trends and challenges for simultaneous multifunction control. J Neural Eng 11:051001

Ivanenko YP, Poppele RE, Lacquaniti F (2004) Five basic muscle activation patterns account for muscle activity during human locomotion. J Physiol 556:267–282

Kuiken TA, Lowery MM, Stoykov NS (2003) The effect of subcutaneous fat on myoelectric signal amplitude and cross-talk. Prosthet Orthot Int 27:48–54

Kutch JJ, Valero-Cuevas FJ (2011) Muscle redundancy does not imply robustness to muscle dysfunction. J Biomech 44:1264–1270

Kutch JJ, Valero-Cuevas FJ (2012) Challenges and new approaches to proving the existence of muscle synergies of neural origin. PLoS Comput Biol 8:e1002434

Latash ML, Anson JG (2006) Synergies in health and disease: relations to adaptive changes in motor coordination. Phys Ther 86:1151–1160

Lee DD, Seung HS (2001) Algorithms for non-negative matrix factorization. In: Advances in neural information processing systems, pp 556–562

Leib R, Rubin I, Nisky I (2018) Force feedback delay affects perception of stiffness but not action, and the effect depends on the hand used but not on the handedness. J Neurophysiol 120(2):781–794

Levine AJ, Hinckley CA, Hilde KL, Driscoll SP, Poon TH, Montgomery JM, Pfaff SL (2014) Identification of a cellular node for motor control pathways. Nat Neurosci 17:586–593

Liu X, Mosier KM, Mussa-Ivaldi FA, Casadio M, Scheidt RA (2011) Reorganization of finger coordination patterns during adaptation to rotation and scaling of a newly learned sensorimotor transformation. J Neurophysiol 105:454–473

Muceli S, Jiang N, Farina D (2014) Extracting signals robust to electrode number and shift for online simultaneous and proportional myoelectric control by factorization algorithms. IEEE Trans Neural Syst Rehabilit Eng 22:623–633

Mussa-Ivaldi FA, Bizzi E (2000) Motor learning through the combination of primitives. Philoso Trans R Soc B 355:1755–1769

Neptune RR, Clark DJ, Kautz SA (2009) Modular control of human walking: a simulation study. J Biomech 42:1282–1287

Oldfield RC (1971) The assessment and analysis of handedness: the Edinburgh inventory. Neuropsychologia 9:97–113

Osu R, Burdet E, Franklin DW, Milner TE, Kawato M (2003) Different mechanisms involved in adaptation to stable and unstable dynamics. J Neurophysiol 90:3255–3269

Overduin SA, d'Avella A, Carmena JM, Bizzi E (2012) Microstimulation activates a handful of muscle synergies. Neuron 76:1071–1077

Pellegrino L, Coscia M, Muller M, Solaro C, Casadio M (2018) Evaluating upper limb impairments in multiple sclerosis by exposure to different mechanical environments. Sci Rep 8:2110

Perotto A, Delagi EF (2005) Anatomical guide for the electromyographer: the limbs and trunk. Charles C Thomas Publisher

Ranganathan R, Krishnan C (2012) Extracting synergies in gait: using EMG variability to evaluate control strategies. J Neurophysiol 108:1537–1544

Roh J, Rymer WZ, Beer RF (2012) Robustness of muscle synergies underlying three-dimensional force generation at the hand in healthy humans. J Neurophysiol 107:2123–2142

Roh J, Rymer WZ, Perreault EJ, Yoo SB, Beer RF (2013) Alterations in upper limb muscle synergy structure in chronic stroke survivors. J Neurophysiol 109:768–781

Roy EA, Kalbfleisch L, Elliott D (1994) Kinematic analyses of manual asymmetries in visual aiming movements. Brain Cogn 24:289–295

Sainburg RL (2002) Evidence for a dynamic-dominance hypothesis of handedness. Exp Brain Res 142:241–258

Sainburg RL (2005) Handedness: differential specializations for control of trajectory and position. Exerc Sport Sci Rev 33:206–213

Sainburg RL, Schaefer SY (2004) Interlimb differences in control of movement extent. J Neurophysiol 92:1374–1383

Santello M (2002) Kinematic synergies for the control of hand shape. Arch Ital Biol 140:221–228

Sathiamoorthy A, Sathiamoorthy SS (1990) Limb dominance and motor conduction velocity of median and ulnar nerves. Indian J Physiol Pharmacol 34:51–53

Semmler JG, Nordstrom MA (1998) Hemispheric differences in motor cortex excitability during a simple index finger abduction task in humans. J Neurophysiol 79:1246–1254

Steele KM, Tresch MC, Perreault EJ (2015) Consequences of biomechanically constrained tasks in the design and interpretation of synergy analyses. J Neurophysiol 113:2102–2113

Tan U (1989) Spinal motor lateralization assessed by recovery curve of H reflex from wrist flexors in right-, and left-handed normal subjects. Int J Neurosci 48:309–312

Teulings HL, Contreras-Vidal JL, Stelmach GE, Adler CH (1997) Parkinsonism reduces coordination of fingers, wrist, and arm in fine motor control. Exp Neurol 146:159–170

Ting LH, McKay JL (2007) Neuromechanics of muscle synergies for posture and movement. Curr Opin Neurobiol 17:622–628

Ting LH, Chiel HJ, Trumbower RD, Allen JL, McKay JL, Hackney ME, Kesar TM (2015) Neuromechanical principles underlying movement modularity and their implications for rehabilitation. Neuron 86:38–54

Torricelli D, Barroso F, Coscia M, Alessandro C, Lunardini F, Esteban EB, d'Avella A (2016) Muscle synergies in clinical practice: theoretical and practical implications. In: Emerging therapies in neurorehabilitation II. Springer, pp 251–272

Tresch MC, Cheung VC, d'Avella A (2006) Matrix factorization algorithms for the identification of muscle synergies: evaluation on simulated and experimental data sets. J Neurophysiol 95:2199–2212

Tropea P, Monaco V, Coscia M, Posteraro F, Micera S (2013) Effects of early and intensive neuro-rehabilitative treatment on muscle synergies in acute post-stroke patients: a pilot study. J Neuroeng Rehabilit 10:103

van Doorn RR (2008) Manual asymmetries in the temporal and spatial control of aimed movements. Hum Mov Sci 27:551–576

Volkmann J, Schnitzler A, Witte OW, Freund H (1998) Handedness and asymmetry of hand representation in human motor cortex. J Neurophysiol 79:2149–2154

Wang J, Sainburg RL (2007) The dominant and nondominant arms are specialized for stabilizing different features of task performance. Exp Brain Res 178:565–570

Washabaugh EP, Krishnan C (2018) A wearable resistive robot facilitates locomotor adaptations during gait. Restor Neurol Neurosci 36:215–223

Woodworth RS (1899) Accuracy of voluntary movement. Psychol Rev 3:i

Yakovenko S, Krouchev N, Drew T (2011) Sequential activation of motor cortical neurons contributes to intralimb coordination during reaching in the cat by modulating muscle synergies. J Neurophysiol 105:388–409

Zardoshti-Kermani M, Wheeler BC, Badie K, Hashemi RM (1995) EMG feature evaluation for movement control of upper extremity prostheses. IEEE Trans Rehabilit Eng 3:324–333